SAND2015-9127J

Cyclotron resonance spectroscopy of a high-mobility two-dimensional electron gas from 0.4 to 100 K at high filling factors

Jeremy A. Curtis,[1] Takahisa Tokumoto,[1] Judy G. Cherian,[2] Junichiro Kono,[3] John L. Reno,[4] Stephen A. McGill,[2] Denis Karaiskaj,[5] and David J. Hilton[1]

[1] *Department of Physics, University of Alabama at Birmingham, Birmingham, AL 35294-1170 USA*
[2] *National High Magnetic Field Laboratory, Florida State University, Tallahassee, FL 30201 USA*
[3] *Department of Electrical and Computer Engineering, Rice University, Houston, TX 77006 USA*
[4] *Center for Integrated Nanotechnologies, Sandia National Laboratory, Albuquerque, NM 87185 USA*
[5] *Department of Physics, University of South at Florida, Tampa, FL 33620 USA*

We have studied the cyclotron mobility of a Landau-quantized two-dimensional electron gas as a function of temperature ($0.4 - 100\,\mathrm{K}$) at a fixed magnetic field ($1.25\,\mathrm{T}$) using terahertz time-domain spectroscopy in a sample with a low frequency mobility of $\mu_{dc} = 3.6 \times 10^6\,\mathrm{cm^2\,V^{-1}\,s^{-1}}$ and a carrier concentration of $n_s = 2 \times 10^6\,\mathrm{cm^{-2}}$. The low temperature mobility in this sample results from both impurity scattering and acoustic deformation potential scattering, with $\mu_{CR}^{-1} \approx \left(2.1 \times 10^5\,\mathrm{cm^2\,V^{-1}\,s^{-1}}\right)^{-1} + \left(3.8 \times 10^{-8}\,\mathrm{V\,s\,K^{-1}\,cm^{-2}} \times T\right)^{-1}$ at low temperatures. Above $50\,\mathrm{K}$, the cyclotron oscillations show a strong reduction in both the oscillation amplitude and lifetime that is dominated by the contribution due to polar optical phonons. These results suggest that electron dephasing times as long as $\sim 300\,\mathrm{ps}$ are possible even at this high filling factor ($\nu = 6.6$) in higher mobility samples ($> 10^7\,\mathrm{cm^2\,V^{-1}\,s^{-1}}$) that have lower impurity concentrations and where the cyclotron mobility at this carrier concentration would be limited by acoustic deformation potential scattering.

PACS numbers: Cyclotron resonance, condensed matter, 76.40.+b, Landau levels, 71.70.Di, Quantum wells, 78.67.De.

I. INTRODUCTION

The gallium arsenide two-dimensional electron gas has long been used as a model system to study of electronic transport in two-dimensional systems to study the fundamental limits of materials physics[1–6]. New device geometries that exploit quantum interference in these samples provide an additional degree of freedom that is increasingly important as devices with ever smaller feature sizes are developed[7–9]. These may also form the basis of next generation quantum logic provided electron coherence lifetimes that are sufficiently long can be achieved[10,11]. Long coherence lifetimes exceeding 6 sec have been achieved using isolated single spins in semiconductor hosts[12], which greatly exceeds lifetimes available in two-dimensional semiconductor materials by several orders of magnitude. Existing coherence times in two-dimensional electron systems are, however, sufficient to demonstrate prototype electronic and optical control of coherence[10,13,14]. The understanding and mitigation of decoherence in these high quality two-dimensional systems will enable a wider array of device geometries based on semiconductor systems and the development of materials with even longer coherence lifetimes will increase the utility of these materials.

Recent interest in monolayer two-dimensional materials include Group IV compounds includes graphene[15,16], silicene[17,18] and germanene[19] as well as transition metal dichalcogenides (MoS_2, $MoSe_2$, WS_2, and WSe_2)[20,21]. The currently available sample mobilities that can be obtained is relatively low when compared to GaAs, with mobilities in multilayer MoS_2, for example, of $\mu_{dc} = 4200\,\mathrm{cm^2\,V^{-1}\,s^{-1}}$ at $30\,\mathrm{K}$ recently reported in Ref. 21. In contrast, theoretical calculations in graphene predict $\mu_{dc} \geq 10^5\,\mathrm{cm^2\,V^{-1}\,s^{-1}}$ at room temperature due to the reduction of long-range polar optical phonon scattering[22]. This mobility would be a substantial enhancement over materials used in conventional electronics[23], which makes graphene and other monolayer materials interesting candidates for future electronics.

The development of these new high-mobility materials will require new spectroscopies that can be used to characterize and elucidate the processes that govern transport in these materials. In this manuscript, we study the temperature dependence of dephasing in a high mobility two dimensional electron gas at $1.25\,\mathrm{T}$ from $0.4\,\mathrm{K}$ to $100\,\mathrm{K}$ using terahertz time-domain spectroscopy. Above $50\,\mathrm{K}$, we observe a rapid dephasing and reduction in cyclotron resonance amplitude that coincides with the onset of strong polar optical phonon scattering in gallium arsenide. Below $1.5\,\mathrm{K}$, we observe an increase in the cyclotron resonance mobility, μ_{CR}, that is limited by remote ionized impurity scattering ($\mu_i = 2.1 \times 10^5\,\mathrm{cm^2\,V^{-1}\,s^{-1}}$), with a weak temperature dependence due to acoustic deformation potential scattering, $\mu_A = \left(\alpha T\right)^{-1}$, with a temperature coefficient given by $\alpha = 3.5 \times 10^{-8}\,\mathrm{V\,s\,K^{-1}\,cm^{-2}}$. These results suggest that it is possible to achieve dephasing times on the order of $\sim 300\,\mathrm{ps}$ at this filling factor in higher mobility samples where the contribution from impurity scattering is minimized and dephasing is limited by acoustic deformation potential scattering[3].

Cyclotron resonance is a well-established experimental technique that measures the temperature and magnetic field dependence of the electronic and optical properties

in bulk[24] and quantum-confined semiconductors[25–28]. The magnetic field, $\vec{B} = B_0\hat{z}$, splits the density of states near the Fermi energy, E_F, into quantized Landau levels separated by the cyclotron energy ($h\nu_c = \hbar eB_0/m^*$)[29,30]. In the experimental data acquired in these experiments, the resonance frequency, ν_c, determines the effective mass, m^*, of carriers in the 2D layer while the resonance line width, $\Delta\nu$, and amplitude, A, are both functions of the dephasing time, τ_{CR}, and the carrier concentration, n_s[27].

Cyclotron resonance has been extensively used to study the dynamic properties of two-dimensional electron systems in external magnetic fields. Reference 25 observed a filling factor dependent change in the cyclotron resonance line width at 5 K that they attributed to the reduced intra-Landau level scattering when the E_F is between Landau levels. A series of cyclotron resonance experiments in samples with a range of mobilities from $\mu_{dc} = 1.2\times10^5\,\mathrm{cm^2\,V^{-1}\,s^{-1}}$ to $1\times10^6\,\mathrm{cm^2\,V^{-1}\,s^{-1}}$ observed line width maxima at even filling factors due to impurity scattering as well as several rational fractions ($\frac{5}{3}$, $\frac{4}{3}$, and $\frac{2}{3}$) due to reduced screening, although the line width oscillations were more prominent in the *lower* mobilities samples[31]

The onset of strong Coulomb repulsions were first observed as an anomalous shift in the cyclotron resonance frequency due to an enhancement in the effective mass in a sample with $\mu_{dc} = 6.7\times10^4\,\mathrm{cm^2\,V^{-1}\,s^{-1}}$ in Ref. 32. Subsequent investigations with higher mobility samples ($\sim 10^5\,\mathrm{cm^2\,V^{-1}\,s^{-1}}$) in Ref. 26 reported a similar red shift in the cyclotron frequency and demonstrate that it can be controlled by both the carrier concentration and external magnetic field. Reference 27 studied a range of carrier concentrations for $1.55\times10^{10}\,\mathrm{cm^{-2}}$ to $1.0\times10^{11}\,\mathrm{cm^{-2}}$ in a sample with a mobility of $3\times10^5\,\mathrm{cm^2\,V^{-1}\,s^{-1}}$ and determined a dephasing time of 104 ps at this low filling factor ($\nu = 0.4$). The authors note, however, the *absence* of cyclotron resonance line width oscillations, which they attribute to the saturation of the intensity transmission line width in high mobility samples ($\geq 10^5\,\mathrm{cm^2\,V^{-1}\,s^{-1}}$), which eventually becomes independent of any change to the cyclotron resonance mobility, μ_{CR}. Because of this saturation effect, few systematic investigations of the cyclotron line width (μ_{CR}) have been performed, despite the significant interest in the development of long-coherence lifetimes semiconductor systems for device applications.

II. EXPERIMENT DETAILS

Terahertz time-domain spectroscopy is a new implementation of cyclotron resonance that uses broadband subpicosecond terahertz pulses and a fixed $\vec{B}$[34–38] instead of a fixed wavelength source with a variable $\vec{B}$[39]. Prior generations of cyclotron resonance experiments measure the intensity of the transmitted far infrared or terahertz light and have known limitations in the highest

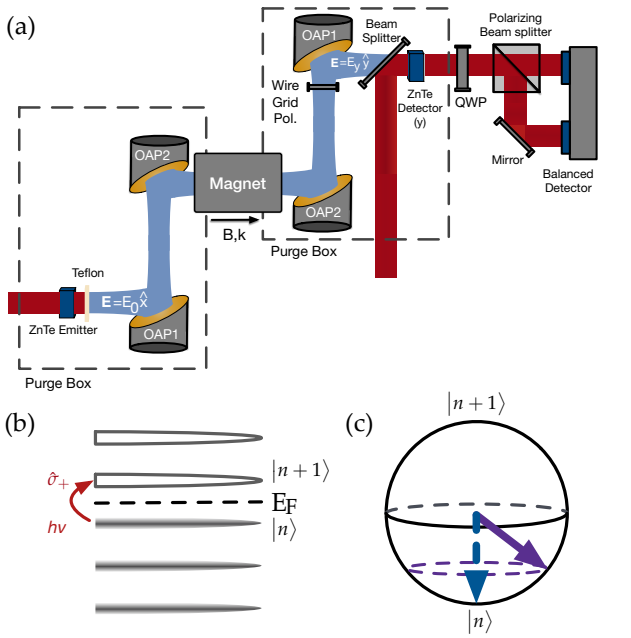

FIG. 1. (a) The apparatus used in the experiments and described in this manuscript is shown here[33]. Both the emitter and detector are zinc telluride (ZnTe), emitting linearly polarized terahertz pulses ($\hat{x}$). The detector is aligned to measure the cross polarized component ($\hat{y}$) of the terahertz electric field that is generated by $\vec{B}$. (OAP = Off-axis parabolic mirror, QWP = Quarter wave plate) (b) The application of an external magnetic field results in the formation of a spectrum of discrete Landau levels separated by the cyclotron energy, $h\nu_c$. Adjacent levels have dipole-allowed optical transitions coupled by a circular polarized component of electromagnetic field[29,30]. This results in both circular dichroism (elliptical polarization) and circular birefringence (field rotation) in the 2DEG and modifies the polarization of the transmitted terahertz pulse near ν_c. (c) A Bloch sphere representation of the two-level system model used to describe our experiments, where the south pole is the highest filled Landau level ($|n\rangle$), the north pole is the lowest unfilled level ($|n+1\rangle$).

mobility samples. The resonance line width, $\Delta\nu$, saturates in samples with $\mu_{dc} \geq 10^5\,\mathrm{cm^2\,V^{-1}\,s^{-1}}$ and does not unambiguously determine the dephasing time, τ_{CR} (see Ref. 27 for a further discussion of this "saturation effect"). Phase-sensitive detection methods, which we employ in our experiments, can directly determine the frequency-dependent real and imaginary dielectric constants ($\tilde{\chi}(\nu)$ in this manuscript) in a single experimental measurement and, thus, overcome these limitations[34–38].

Figure 1(a) shows a diagram of our cyclotron resonance experiment. An 800 nm pulse from a titanium:sapphire laser amplifier (Coherent Legend) with duration of 0.150 ps and an energy of 0.6 mJ is used to produce near-single cycle terahertz pulses by optical rectification in 1 mm thick (110)-oriented zinc telluride (Ingcrys Laser Systems)[40]. The resulting subpicosecond pulse is linearly polarized ($\vec{E} = E_0\hat{x}$) with a spectrum of

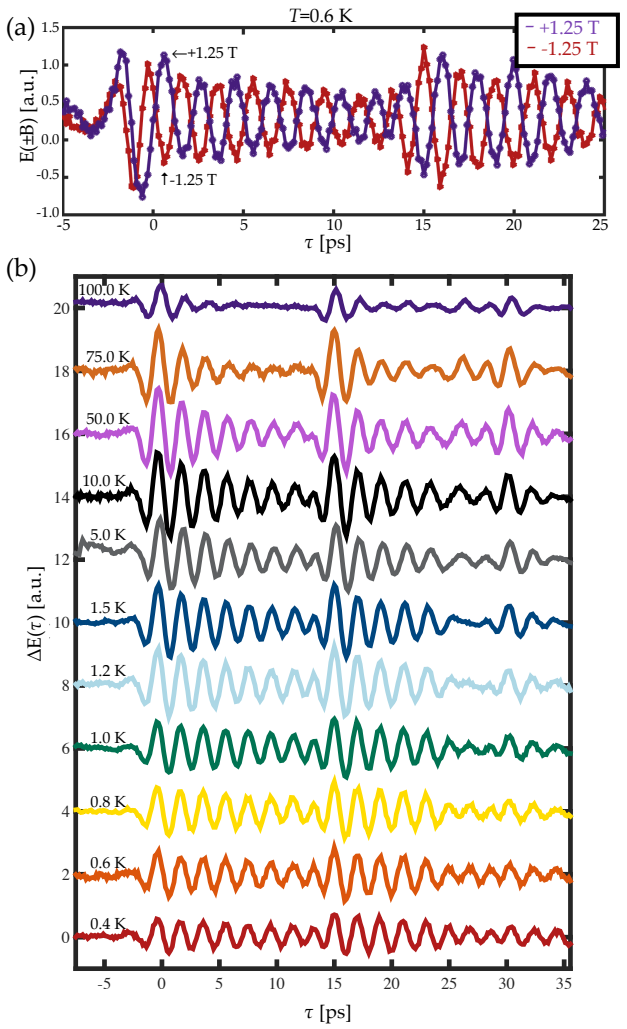

FIG. 2. (a) Cyclotron resonance data that show oscillations at ±1.25 T and at 0.6 K are shown here. (b) Cyclotron resonance data for temperatures from 0.4 K (bottom curve) to 100 K (top curve), showing the increase in dephasing time at low temperatures. Data shown here at 0.6 K also appear in their subtracted form in Fig. 2(a). The fitting of these data to the multilayer transmission model described in the text results and in Ref. 38 will be shown in Fig. 3. Secondary pulse located at approximately ∼ 15 ps results from multiple reflections within the GaAs substrate.

frequencies from 0.2 to 1.2 THz. The terahertz pulse has a fluence that is $\ll 1\,\mathrm{nJ\,cm^{-2}}$, which results in negligible sample heating in all of our experiments. This terahertz pulse is normally incident ($\theta = 0$) on the 2DEG sample in a 10 T superconducting magnet (Oxford Instruments SpectroMag) with $\vec{B} \parallel \vec{k}$, where $\vec{k} = \kappa\hat{z}$ is the propagation vector of the terahertz pulse. This magnet has a Helium-3 cryostat and a base temperature of 0.4 K.

A 2DEG in a perpendicular magnetic field results in a transmitted terahertz pulse that is elliptically polarized with components along both $\hat{x}$ and $\hat{y}$ due to in the magnetic field-induced circular dichroism. We use standard electro-optic sampling techniques to record the amplitude and phase of one linearly polarized component of the transmitted pulse[41]. The polarization axis ($\hat{y}$) of the detector is aligned to measure the cross polarized component induced by the applied magnetic field. To improve the polarization extinction of this detector configuration, we also align a wire grid polarizer (Microtech Instruments, Model G30) along the $\hat{y}$ direction. This entire experiment is performed in a dry nitrogen atmosphere to minimize the effects of water vapor absorption on our data[42].

Our experiments study a 30 nm thick modulation doped single GaAs quantum well (sample: EA0745) grown via molecular beam epitaxy. Electrons in this quantum well are generated by a pair of δ-doped silicon monolayers with setback distances of 77.6 nm and 99.3 nm. This geometry results in a carrier concentration of $n_s = 2 \times 10^{11}\,\mathrm{cm^{-2}}$ and a mobility of $\mu_{dc} = 3.6 \times 10^6\,\mathrm{cm^2\,V^{-1}\,s^{-1}}$ at 4.2 K . This combination of magnetic field and carrier concentration results in a filling factor of $\nu = 2n_s\sqrt{\hbar e^{-1}B_0^{-1}} = 6.6$ for all experiments described in this manuscript.

III. DATA AND ANALYSIS

We measure the terahertz waveform as a function of temperature at both $B_0 = \pm 1.25$ T and subtract them to isolate the component of the terahertz electric field that demonstrates broken time-reversal symmetry by undergoing a π phase change on magnetic field reversal[43,44]. A representative set of data is shown in Fig. 2(a) for ±1.25 T at 0.6 K. The time-delayed pulses that appear at multiples of ∼ 15 ps after the initial pulse are additional Fabry-Perot reflections from the 625 μm gallium arsenide substrate on which the sample is grown. Figure 2(b) shows the subtracted data (offset vertically for clarity) as a function of temperature from 0.4 K to 100 K, showing an increase in oscillation lifetime as temperature is lowered and a reduction in oscillation amplitude below 1.5 K and also above 50 K.

Transmission through a multilayer sample can be modeled using the Characteristic matrix method[45,46], which we have previously extended in Ref. 38 to include materials, like in the present study, that are in external magnetic field. A brief summary of this analysis technique is included here. The thickness, z_j, and admittance, $Y_j = n_j Y_0$, describe the j-th layer of the multilayer 2DEG, where n_j is the refractive index and $Y_0 = \sqrt{\epsilon_0/\mu_0}$ is the admittance of free space. $\mathbb{M}_{\pm,j}$ for this layer and for one circular polarization component, $\hat{\sigma}_\pm = \frac{1}{\sqrt{2}}(\hat{x} \pm i\hat{y})$, is given by:

$$\overline{\mathbb{M}}_{\pm,j} \doteq \begin{bmatrix} \cos(\kappa_{\pm,j} z_j) & \pm Y_\pm^{-1} \sin(\kappa_{\pm,j} z_j) \\ \mp Y_\pm \sin(\kappa_{\pm,j} z_j) & \cos(\kappa_{\pm,j} z_j) \end{bmatrix} \qquad (1)$$

where $\kappa_{\pm,j} = 2\pi\nu n_j \lambda^{-1}$ is the wave number. The full Characteristic matrix, $\mathbb{M}_\pm = \prod_j \mathbb{M}_{\pm,j} \doteq \left[\begin{smallmatrix} A & B \\ C & D \end{smallmatrix}\right]$, for the

multilayer structure is given by the product of the individual $\overline{\mathbb{M}}_{\pm,j}$. The transmission coefficient, $\tilde{t}_{\pm}$, for each polarization is given by:

$$\tilde{t}_{\pm}(\nu) = \frac{2}{\left(A + Y_t Y_i^{-1} D\right) \pm i\left(Y_i^{-1} C - Y_t B\right)} \tag{2}$$

where Y_t and Y_i are the admittance of the transmitted and incident medium, respectively. This method allows us to model the entire cyclotron resonance signal shown in Fig. 2(b), including the present case when the oscillation time is long and there is interference between the multiple reflections[35,47].

We use a two-level system approximation for the susceptibility, $\tilde{\chi}(\nu)$, of the cyclotron-active polarization component that results from splitting the density of states near E_F. This neglects all Landau levels except for the highest filled level ($|n\rangle$) and lowest unfilled level ($|n+1\rangle$) near E_F and is appropriate for the dipole ($\hat{d}$) transitions that we can access with the low terahertz pulse energies in our experiment. The terahertz pulse results in an ensemble of coherently coupled two-level systems, represented as a vector on the Bloch sphere in Fig. 1(c). The dynamical $\tilde{\chi}(\nu)$ of this two-level system in SI units is a homogeneously broadened absorption line given by:

$$\tilde{\chi}(\nu) = \left(\frac{1}{\epsilon_0 \hbar} N \left|\hat{d}\right|^2 \tau_{CR}\right)\left[\frac{i - 2\pi(\nu - \nu_c)\tau_{CR}}{1 + 4\pi^2(\nu - \nu_c)^2 \tau_{CR}^2}\right] \tag{3}$$

where N is the population in $|n\rangle$ before the terahertz pulse excitation and $\left|\hat{d}\right|^2$ is the square dipole transition matrix element for the $|n\rangle \rightarrow |n+1\rangle$ transition[48]. This $\tilde{\chi}(\nu)$ corresponds to a causal response function, $R(t)$, in the time-domain that is given by eq. (4), where IFT is the inverse Fourier transform operation[38,49] and $\mathrm{u}(t)$ is the step function.

$$\begin{aligned} R(t) &\equiv \mathrm{IFT}\left[\tilde{\chi}(\nu)\right] \\ &= \left(\frac{2}{\epsilon_0 \hbar} N \left|\hat{d}\right|^2\right) \mathrm{u}(t) \exp\left(\frac{-t}{\tau_{CR}}\right) \sin 2\pi\nu_c t \end{aligned} \tag{4}$$

For later use in Fig. 3, we define $\tilde{\chi}_0$ to be the maximum value of the imaginary part (absorption) of $\tilde{\chi}$ in eq. (5a), which occurs at $\nu = \nu_c$. Likewise, the peak amplitude of this causal response is given by eq. (5b) using the same parameters as the $\tilde{\chi}$ model.

$$\tilde{\chi}_0 = \frac{1}{\epsilon_0 \hbar} N \left|\hat{d}\right|^2 \tau_{CR} \tag{5a}$$

$$A = \frac{2}{\epsilon_0 \hbar} N \left|\hat{d}\right|^2 \tag{5b}$$

We determine the best-fit to our data using a constrained genetic algorithm in MATLAB with the Characteristic matrix model for $\tilde{t}(\nu)$ and two-level approximation for $\tilde{\chi}(\nu)$. Figure 3(a) shows $\tilde{\chi}_0$ for each of our

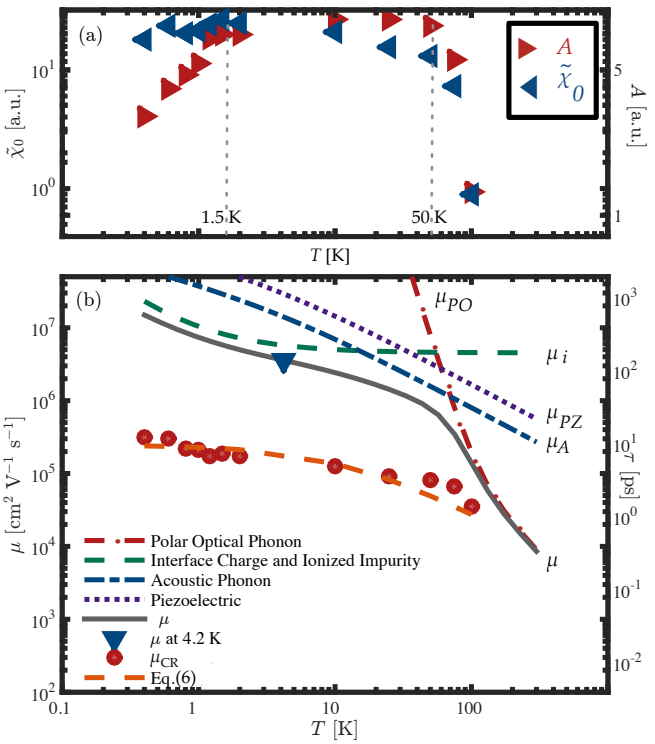

FIG. 3. (color online) (a) (▶, right axis): The amplitude of the time-domain oscillations, A, is presented as a function of temperature. (◀, left axis): The magnitude of the susceptibility, $\tilde{\chi}_0$, is presented as a function of temperature. (b) (●, right axis): The cyclotron mobility, μ_{CR}, in EA0745 is shown here, with the same data presented using the dephasing time, τ_{CR}, on the opposite axis (●, right axis). (▼): The low frequency mobility at 4.2 K was determined using transport characterization techniques. (−, left axis): The mobility is calculated using Matthiessen's rule from the individual contributions, using the equations taken from Ref. 50. (−−, left axis): The polar optical phonon scattering contribution is given by eq. (31) in Ref. 50. (−−, left axis): The combined remote ionized impurity scattering and interface charge contribution, which is given by eqs. (26) and (28) in Ref. 50. (−·, left axis): The contribution due to acoustic phonon scattering, which is given by eq. (34) in Ref. 50. (···, left axis): The contribution due to piezoelectric scattering, which is given by eq. (37) in Ref. 50.

temperatures (◀, left axis), with an approximately temperature independent behavior below 10 K and a rapid decrease as temperature is increased above 50 K. This is in contrast to the amplitude, A, which is also shown on Fig. 3(a) (▶, right axis), which decrease below 1.5 K, as will be discussed in more detail below. We note that the terahertz beam waist at the sample position has a diameter that is comparable to the sample dimensions and probe aperture, which potentially makes our result sensitive to changes in the system alignment including a temperature dependent change to the insert probe length. We have verified this does not contribute to the reduction in A below 1.5 K by measuring the transmission through

the magnet absent a sample and noting no reduction in signal throughout the temperature range studied.

Figure 3(b) plots the dephasing time (τ_{CR}) as a function of sample temperature (•, right axis) and, also, converted to a mobility using $\mu_{CR} = e\tau_{CR}/m^*$ (•, left axis), which monotonically increases as the temperature is lowered from 100 K to 0.4 K in our experiments. The cyclotron oscillation frequency, $\nu_c = 0.516$ THz, determined by this fitting is consistent with an effective mass of $m^* = 0.0678m_0$, where m_0 is the free electron mass. This is within $\sim 0.5\%$ of the accepted value the effective mass of gallium arsenide[51] and does not show enhancement at our high filling factor ($\nu = 6.6$)[26].

IV. RESULTS AND DISCUSSION

Figure 3(b) shows a simulation of μ_{dc} as a function of temperature for our carrier concentration using the model described in Ref. 50. The lattice contributions to μ_{dc} include polar optical phonon scattering (μ_{PO}, $-\cdot-$), piezoelectric scattering (μ_{PZ}, $\cdot\cdot\cdot$), and acoustic deformation potential scattering (μ_A, $-\cdot$). In addition to these, impurity scattering (μ_i, $--$) results from both the contributions due to remote ionized impurity scattering (μ_{RI}) and surface charge scattering (μ_{BI}). As was also the case in Ref. 50, the interface charge density, N_{BI} and remote ionized impurity concentration, N_i, are not independently known in our sample. Samples with $\mu_{dc} \geq 10^6\,\mathrm{cm^2\,V^{-1}\,s^{-1}}$ grown using molecular beam epitaxy, however, typically have impurity concentrations of $n_i \leq 10^{14}\,\mathrm{cm^{-3}}$, which allows us to estimate the combined contribution to $\mu_i^{-1} = \mu_{RI}^{-1} + \mu_{BI}^{-1}$ in this sample ($--$). The full mobility, μ_{dc}, is then calculated using Matthiessen's rule ($\mu_{dc}^{-1} = \mu_{PO}^{-1} + \mu_{PZ}^{-1} + \ldots$) using the individual contributions to fit our measured mobility at 4.2 K (▼).

The amplitude of the cyclotron oscillations is approximately constant between 1.5 K and 50 K, with significant decreases both above and below this range. At the highest temperatures studied, the decrease in the value of A corresponds to the onset of strong polar optical phonon scattering[2,52] as the main contribution to μ_{dc} and results in rapid dephasing of the ensemble coherence on a time scale comparable to the terahertz pulse width[53]. At temperatures below 1.5 K, the amplitude is a direct measure of the reduction of $N\left|\hat{d}\right|^2$, as noted in eq. (5b)[54]. This indicates either a reduction in the population N or a modification to the dipole matrix element, $\left|\left\langle n\middle|\hat{d}\middle|n+1\right\rangle\right|$. The carrier population in this modulation doped sample originates from the spatially separated δ-doped silicon layer to avoid freeze out of the carriers[55]. We also note that prior investigations of 2DEG samples with lower mobilities did not observed a reduction in population[27,32]. A full explanation of this reduction in A will require additional experiments to study the temperature and magnetic field dependence of cyclotron resonance in this high mobility sample.

At the lowest temperatures, we fit our μ_{CR} to a simplified model using a low temperature approximation to Matthiessen's rule:

$$\mu_{CR}^{-1} \simeq \mu_i^{-1} + \alpha T + \ldots \tag{6}$$

where μ_i is the contribution to remote ionized impurities. The contribution due to acoustic deformation potential scattering, $\mu_A = \left(\alpha T\right)^{-1}$, should be the significant temperature-dependent contribution at this n_s based on the results shown in Fig. 3(b)[53,56]. We find a best-fit to our data using $\alpha = 3.8 \times 10^{-7}\,\mathrm{V\,s\,K^{-1}\,cm^{-2}}$ and $\mu_i = 2.1 \times 10^5\,\mathrm{cm^2\,V^{-1}\,s^{-1}}$, which is included on Fig. 3(b) (——). A theoretical calculation of the acoustic deformation potential mobility in gallium arsenide at $B = 0$ found a value of $\alpha = 3.5 \times 10^{-8}\,\mathrm{V\,s\,K^{-1}\,cm^{-2}}$ in samples with a similar carrier concentration ($n_s = 0.2 - 2 \times 10^{11}\,\mathrm{cm^{-2}}$) in Ref. 3. That value of α is an order of magnitude smaller than the value determined in our work, likely resulting from the modification of the density of states and wavefunctions near the Fermi surface due to the Landau quantization.

Our α allows us to estimate the dephasing time that would be possible in high mobility gallium arsenide samples where the contribution due to remote ionized impurities is minimized and acoustic deformation potential scattering would be expected to limit μ (Ref. 3). From our data, the cyclotron mobility at 0.4 K would be $\mu_A = 6.6 \times 10^6\,\mathrm{cm^2\,V^{-1}\,s^{-1}}$ at this filling factor, which would correspond to a dephasing time on the order of ~ 300 ps. We note that lower filling factors are also possible at higher magnetic fields or lower n_s, which have shown in prior experiments increase τ_{CR}[25–27,31].

V. CONCLUSIONS

In summary, we have performed cyclotron resonance spectroscopy in a Landau-quantized two dimensional electron gas with a high mobility of $3.6 \times 10^6\,\mathrm{cm^2\,V^{-1}\,s^{-1}}$ and a carrier concentration of $n_s = 2 \times 10^{10}\,\mathrm{cm^{-2}}$. We find a cyclotron resonance mobility, μ_{CR}, of $3.2 \times 10^5\,\mathrm{cm^2\,V^{-1}\,s^{-1}}$ at 0.4 K and determine a fitting to our low temperature cyclotron mobility given by $\mu_{CR}^{-1} = \mu_i^{-1} + \left(\alpha T\right)^{-1}$ with $\alpha = 3.5 \times 10^{-8}\,\mathrm{V\,s\,K^{-1}\,cm^{-2}}$ and $\mu_i = 2.1 \times 10^5\,\mathrm{cm^2\,V^{-1}\,s^{-1}}$. These results predict that coherence lifetimes on the order of 300 ps are possible in higher mobility samples and at this filling factor. Future work will focus on studying this material at lower filling factors to study line width oscillations and the potential for effective mass enhancement as well as to elucidate the observed reduction in cyclotron resonance amplitude below 1.5 K.

VI. ACKNOWLEDGEMENTS

This material is based upon work supported by the National Science Foundation under Grant No. DMR-

1056827 (JAC, TT, and DJH) and DMR-1409473 (DK). JAC also acknowledges support from the U.S. Dept. Education GAANN Fellowship (P200A090143). A portion of this work was performed at the National High Magnetic Field Laboratory, which is supported by National Science Foundation Cooperative Agreement No. DMR-1157490 and the State of Florida. This work was performed, in part, at the Center for Integrated Nanotechnologies, a U.S. Department of Energy, Office of Basic Energy Sciences user facility at Los Alamos National Laboratory (Contract DE-AC52-06NA25396) and Sandia National Laboratories (Contract DE-AC04-94AL85000).

[1] Tsuneya Ando, Alan B Fowler, and Frank Stern, "Electronic properties of two-dimensional systems," Reviews of Modern Physics **54**, 437–672 (1982).

[2] B J F Lin, D C Tsui, M A Paalanen, and A C Gossard, "Mobility of the two-dimensional electron gas in GaAs-AlxGa1-xAs heterostructures," Applied Physics Letters **45**, 695 (1984).

[3] J J Harris, C T Foxon, D Hilton, J Hewett, C Roberts, and S Auzoux, "Acoustic phonon scattering in ultra-high mobility, low carrier density GaAs/(Al,Ga)As heterojunctions," Surface Science **229**, 113–115 (1990).

[4] O E Dial, R C Ashoori, L N Pfeiffer, and K W West, "High-resolution spectroscopy of two-dimensional electron systems," Nature **448**, 176 (2007).

[5] Thierry Champel, Serge Florens, and L Canet, "Microscopics of disordered two-dimensional electron gases under high magnetic fields: Equilibrium properties and dissipation in the hydrodynamic regime," Physical Review B **78**, 125302 (2008).

[6] S Das Sarma, E H Hwang, S Kodiyalam, L N Pfeiffer, and K W West, "Transport in two-dimensional modulation-doped semiconductor structures," Physical Review B **91**, 205304 (2015).

[7] Yang Ji, Yunchul Chung, D Sprinzak, M Heiblum, D Mahalu, and Hadas Shtrikman, "An electronic Mach Zehnder interferometer," Nature **422**, 415–418 (2003).

[8] Ivan P Levkivskyi and Eugene V Sukhorukov, "Dephasing in the electronic Mach-Zehnder interferometer at filling factor ν=2," Physical Review B **78**, 045322 (2008).

[9] L V Litvin, A Helzel, H P Tranitz, W Wegscheider, and C Strunk, "Edge-channel interference controlled by Landau level filling," Physical Review B **78**, 075303 (2008).

[10] Angik Sarkar, T K Bhattacharyya, and Ajay Patwardhan, "Quantum logic processor: Implementation with electronic Mach-Zehnder interferometer," Applied Physics Letters **88**, 213113 (2006).

[11] T D Ladd, F Jelezko, R Laflamme, Y Nakamura, C Monroe, and J L O'Brien, "Quantum computers," Nature **464**, 45–53 (2010).

[12] Andrea Morello, Jarryd J Pla, Floris A Zwanenburg, Kok W Chan, Kuan Y Tan, Hans Huebl, Mikko Möttönen, Christopher D Nugroho, Changyi Yang, Jessica A van Donkelaar, Andrew D C Alves, David N Jamieson, Christopher C Escott, Lloyd C L Hollenberg, Robert G Clark, and Andrew S Dzurak, "Single-shot readout of an electron spin in silicon," Nature **467**, 687–691 (2010).

[13] N Bonadeo, J Erland, D Gammon, D Park, D Katzer, and D Steel, "Coherent Optical Control of the Quantum State of a Single Quantum Dot," Science **282**, 1473 (1998).

[14] T Arikawa, X Wang, David J Hilton, J L Reno, W Pan, and J Kono, "Quantum control of a Landau-quantized two-dimensional electron gas in a GaAs quantum well using coherent terahertz pulses," Physical Review B **84**, 241307 (2011).

[15] M L Sadowski, G Martinez, M Potemski, C Berger, and W De Heer, "Landau level spectroscopy of ultrathin graphite layers," Physical Review Letters **97**, 266405 (2006).

[16] A K Geim and K S Novoselov, "The rise of graphene," Nature Materials **6**, 183–191 (2007).

[17] Patrick Vogt, Paola De Padova, Claudio Quaresima, Jose Avila, Emmanouil Frantzeskakis, Maria Asensio, Andrea Resta, Bénédicte Ealet, and Guy Le Lay, "Silicene: Compelling Experimental Evidence for Graphenelike Two-Dimensional Silicon," Physical Review Letters **108**, 155501 (2012).

[18] Li Tao, Eugenio Cinquanta, Daniele Chiappe, Carlo Grazianetti, Marco Fanciulli, Madan Dubey, Alessandro Molle, and Deji Akinwande, "Silicene field-effect transistors operating at room temperature," Nature Nanotechnology **10**, 227–231 (2015).

[19] Elisabeth Bianco, Sheneve Butler, Shishi Jiang, Oscar D Restrepo, Wolfgang Windl, and Joshua E Goldberger, "Stability and Exfoliation of Germanane: A Germanium Graphane Analogue," ACS Nano **7**, 4414–4421 (2013).

[20] Kin Fai Mak, Changgu Lee, James Hone, Jie Shan, and Tony F Heinz, "Atomically Thin MoS_2: A New Direct-Gap Semiconductor," Physical Review Letters **105**, 136805 (2010).

[21] J H Strait, P Nene, and F Rana, "High intrinsic mobility and ultrafast carrier dynamics in multilayer metal-dichalcogenide MoS 2," Physical Review B (2014).

[22] E H Hwang and S Das Sarma, "Acoustic phonon scattering limited carrier mobility in two-dimensional extrinsic graphene," Physical Review B **77**, 115449 (2008).

[23] For example, the electron mobility of unstrained silicon used in current microelectronics is $\mu_{dc} = 1400\,\mathrm{cm}^2\,\mathrm{V}^{-1}\,\mathrm{s}^{-1}$.

[24] J M Luttinger, "Quantum Theory of Cyclotron Resonance in Semiconductors: General Theory," Physical Review **102**, 1030–1041 (1956).

[25] Th Englert, J C Maan, Ch Uihlein, D C Tsui, and A C Gossard, "Observation of oscillatory line width in the cyclotron resonance of GaAs-AlGaAs heterostructures," Solid state communications **46**, 545–548 (1983).

[26] Z Schlesinger, W Wang, and A H MacDonald, "Dynamical Conductivity of the GaAs Two-Dimensional Electron Gas at Low Temperature and Carrier Density," Physical Review Letters **58**, 73–76 (1987).

[27] M Chou, D Tsui, and G Weimann, "Cyclotron resonance of high-mobility two-dimensional electrons at extremely low densities," Physical Review B **37**, 848–854 (1988).

[28] Takahiro Morimoto, Yasuhiro Hatsugai, and Hideo Aoki, "Optical Hall Conductivity in Ordinary and Graphene Quantum Hall Systems," Physical Review Letters **103**, 116803 (2009).

[29] V Fock, "Bemerkung zur Quantelung des harmonischen Oszillators im Magnetfeld," Zeitschrift für Physik **47**, 446–448 (1928).

[30] Claude Cohen-Tannoudji, Bernard Diu, and Frank Laloe, *Quantum Mechanics, Vol. 1*, 1st ed. (Wiley, 1978).

[31] W Seidenbusch, E Gornik, and G Weinmann, "Cyclotron-resonance linewidth oscillations in the integer and fractional quantum Hall regimes," Physical Review B **36**, 9155–9159 (1987).

[32] H Sigg, P Wyder, and J A A J Perenboom, "Analysis of polaron effects in the cyclotron resonance of n-GaAs and AlGaAs-GaAs heterojunctions," Physical Review B **31**, 5253–5261 (1985).

[33] Daniel Mittleman, ed., *Sensing with Terahertz Radiation*, 1st ed. (Springer, Berlin, 2002).

[34] D Some and A V Nurmikko, "Real-time electron cyclotron oscillations observed by terahertz techniques in semiconductor heterostructures," Applied Physics Letters **65**, 3377–3379 (1994).

[35] X Wang, David J Hilton, John L Reno, Daniel M Mittleman, and Junichiro Kono, "Direct measurement of cyclotron coherence times of high-mobility two-dimensional electron gases," Optics Express **18**, 12354–12361 (2010).

[36] Xiangfeng Wang, David J Hilton, L Ren, Daniel M Mittleman, Junichiro Kono, and John L Reno, "Terahertz time-domain magnetospectroscopy of a high-mobility two-dimensional electron gas," Optics Letters **32**, 1845–1847 (2007).

[37] David J Hilton, T Arikawa, T Arikawa, Junichiro Kono, and J Kono, "Cyclotron Resonance," in *Characterization of Materials*, edited by E N Kaufmann (John Wiley and Sons, Inc, New York, 2012) p. 2438.

[38] David J Hilton, "Cyclotron resonance spectroscopy in a high mobility two dimensional electron gas using characteristic matrix methods," Optics Express **20**, 29717–29726 (2012).

[39] See, for example, refs. 26 and 27.

[40] Ajay Nahata, Aniruddha S Weling, and Tony F Heinz, "A wideband coherent terahertz spectroscopy system using optical rectification and electro-optic sampling," Applied Physics Letters **69**, 2321 (1996).

[41] Q Chen, M Tani, Zhiping Jiang, and Xi-Cheng Zhang, "Electro-optic transceivers for terahertz-wave applications," Journal of the Optical Society of America B **18**, 823–831 (2001).

[42] Martin van Exter, Ch Fattinger, and D Grischkowsky, "Terahertz time-domain spectroscopy of water vapor," Optics Letters **14**, 1128–1130 (1989).

[43] C R Brundle, Charles A Evans, and Shaun Wilson, *Encyclopedia of Materials Characterization*, Surfaces, Interfaces, Thin Films (Gulf Professional Publishing, 1992).

[44] O Morikawa, A Quema, S Nashima, H Sumikura, Takeshi Nagashima, and M Hangyo, "Faraday ellipticity and Faraday rotation of a doped-silicon wafer studied by terahertz time-domain spectroscopy," Journal of Applied Physics **100**, 033105 (2006).

[45] Stephen E Ralph, S Perkowitz, N Katzenellenbogen, and D Grischkowsky, "Terahertz spectroscopy of optically thick multilayered semiconductor structures," Journal of the Optical Society of America B: Optical Physics **11**, 2528–2532 (1994).

[46] Max Born and Emil Wolf, *Principles of Optics: Electromagnetic Theory of Propagation, Interference and Diffraction of Light*, 7th ed. (Cambridge University Press, 1999).

[47] L Duvillaret, Frederic Garet, and Jean-Louis Coutaz, "A Reliable Method for Extraction of Material Parameters in Terahertz Time-Domain Spectroscopy ," IEEE Journal of Selected Topics in Quantum Electronics **2**, 739–746 (1996).

[48] Robert W Boyd, *Nonlinear Optics*, 3rd ed. (Academic Press, 2007).

[49] Joseph W Goodman, *Introduction To Fourier Optics*, 2nd ed. (McGraw-Hill Science/Engineering/Math, 1996).

[50] K Lee, M S Shur, T J Drummond, and H Morkoç, "Low field mobility of 2-d electron gas in modulation doped AlxGa1-xAs/GaAs layers," Journal of Applied Physics **54**, 6432 (1983).

[51] Sadao Adachi, "GaAs, AlAs, and AlxGa1-xAs Material parameters for use in research and device applications," Journal of Applied Physics **58**, R1 (1985).

[52] M A Hopkins, R J Nicholas, D J Barnes, M A Brummell, J J Harris, and C T Foxon, "Temperature dependence of the cyclotron-resonance linewidth in GaAs- Ga1-xAlxAs heterojunctions," Physical Review B **39**, 13302–13309 (1989).

[53] T Kawamura and S Das Sarma, "Phonon-scattering-limited electron mobilities in AlxGa1-xAs/GaAs heterojunctions," Physical Review B **45**, 3612–3627 (1992).

[54] In contrast, the $\tilde{\chi}_0$ depends linearly on $N\left|\hat{d}\right|^2\tau_{CR}$ and is approximately constant over the same temperature range.

[55] R Dingle, H L Störmer, A C Gossard, and W Wiegmann, "Electron mobilities in modulation-doped semiconductor heterojunction superlattices," Applied Physics Letters **33**, 665 (1978).

[56] T Kawamura and S Das Sarma, "Temperature dependence of the low-temperature mobility in ultrapure $Al_xGa_{1-x}As$/GaAs heterojunctions: Acoustic-phonon scattering," Physical Review B **42**, 3725–3728 (1990).